Self-demodulation of elastic waves in a one-dimensional granular chain

V. Tournat,* V. E. Gusev, and B. Castagnède
Université du Maine, Avenue Olivier Messiaen, 72085 Le Mans Cedex 9, France
(Received 1 July 2003; revised manuscript received 25 June 2004; published 10 November 2004)

The self-demodulation process in a nonlinear granular chain of identical beads is studied analytically and numerically. In such a medium, in accordance with the dispersion relation, longitudinal waves that have a frequency higher than the so-called cutoff frequency of the chain are evanescent. Here, we study the influence on the self-demodulation process of the transition from the propagative to the evanescent regime in pump wave propagation that takes place when the pump frequency increases. An analytical solution in discrete coordinates is derived for the case of two primary frequencies mixing into a single difference frequency. This solution is then numerically integrated in order to analyze the demodulation of the acoustic wave packet (i.e., of the harmonic acoustic wave modulated in a pulse mode). Temporal demodulated profiles can be strongly sensitive to the regime (propagative or evanescent) of primary wave transport. This model allows us to detect the cutoff frequency of longitudinal elastic waves in the chain, without receiving the primary waves, but receiving the low frequency nonlinearly radiated signal. The roles of frequency dependent attenuation, velocity dispersion, and observation distance are analyzed.

DOI: 10.1103/PhysRevE.70.056603 PACS number(s): 43.25.+y, 45.70.−n, 62.30.+d, 81.70.Cv

I. INTRODUCTION

Although the pioneer theoretical results on nonlinear wave propagation in unidimensional granular chains were obtained 20 years ago [1,2], there is still continuous activity in this domain of research [3–8]. Interest in these studies is supported by the fact that many of the earth's materials and of technological materials are granular and can be tested in real experimental conditions by elastic waves (seismics, underwater acoustics for diagnostics of the sediments, industrial real time monitoring, etc.). Elastic waves have demonstrated powerful capabilities in the control or in the evaluation of these granular materials [13]; however, a better understanding of the characteristic features of wave propagation in such media is needed, especially when scattering, dispersion, absorption, or nonlinear effects occur.

As mentioned in [4], the elastic dynamical behavior of three-dimensional (3D) granular materials represents a complicated problem because it involves a huge number of not well known parameters related, for instance, to the statistical distribution of bead shapes, sizes, constitutive materials, and the contacts between beads, to the geometry of packing, and to the structure of force chains. These features can lead to specific effects in the elastic wave propagation such as noise generation observed in [5], or to a strong sensitivity of sound to temperature variations [6]. In contrast, a simpler realistic problem for both experimental and theoretical studies of elastic wave propagation consists of a 1D chain, made of identical elastic spherical beads in contact. In a sense, the application of a 1D periodic system to model elastic wave propagation in granular materials could seem to be quite rudimentary. However, there is a consensus that the fundamental results obtained in the 1D geometry might be useful for the analysis of 3D problems [4,7]. Moreover, both discrete and nonlinear features that are taken into account in 1D models represent fundamental problems of interest for the general study of nonlinear lattices [8,9]. Here the recent progress in "growth" of regular granular lattices should be mentioned [10–12]

The propagation in granular assemblages is fundamentally nonlinear due to the nonlinearity of the interaction between two adjacent elastic beads, which can be described using the Hertz law [14,15]. The validity of this model for a chain of beads has been tested experimentally (see [4] and the reference therein). One of the first works on the nonlinear effects in 1D granular chains was the propagation of solitonlike pulses [1,2]. Since this time, theoretical, numerical, and experimental studies of soliton collision [16] and backscattering [17], and of the detection of buried impurities using solitons [18] have been performed. In parallel, other nonlinear effects were observed (and modeled) in 3D media, like acoustic wave self-action in geophysics experiments [19], or harmonics generation and self-demodulation in sand [20–22].

Also, such fine linear properties for elastic wave propagation in the longitudinal chain configuration were under active investigation as velocity dispersion [8], scattering by inhomogeneities [17], and shear and Rayleigh wave propagation [8]. In this case, Rayleigh waves are obtained at very high frequencies of longitudinal excitation (the wavelength of the elastic perturbation in the bead's material is smaller than the diameter of the bead). At these high frequencies, other acoustic modes like whispering or breathing can also manifest themselves [23]. For lower frequencies, one of the remarkable predicted and observed features is the transition from propagative longitudinal modes to evanescent modes when the frequency of the waves is increased above the so-called cutoff frequency of the chain [24]. This cutoff frequency depends on a few identified parameters: the longitudinal static stress applied to the chain, the size of the beads, and the elastic properties of the bead material (Young modulus and Poisson ratio). It is also possible to deduce the cutoff

*Electronic address: vincent.tournat@univ-lemans.fr

frequency from the low frequency sound velocity (which depends on the previous parameters) and the bead radius. As a consequence, the cutoff frequency is a source of information on the properties of a granular chain.

One of the experimental difficulties with evanescent waves is that they are attenuated at a distance of several bead diameters, and thus it is often difficult to detect them. We propose a method to obtain information related to the high frequency wave transport modes (propagative or evanescent), using the nonlinear self-demodulation effect produced by a so-called parametric emitting antenna. The first studies of this nonlinear process were performed 50 years ago in the field of underwater acoustics (see [25] and the references therein). Powerful amplitude-modulated high frequency (HF) waves (called primary or pump waves) are radiated first in the nonlinear medium of propagation. Due to the quadratic elastic nonlinearity of the medium, different spectral components of the emitted signal (for example ω_1 and ω_2) interact, to give the sum components $\omega_1+\omega_2, 2\omega_1$, and $2\omega_2$, and also the difference one $\omega_1-\omega_2$. The difference frequency component has a significantly lower frequency than both ω_1 and ω_2 if $|\omega_1-\omega_2| \ll \omega_1, \omega_2$. As the attenuation (from both absorption and scattering) increases with the frequency, only the low frequency (LF) component $\omega_1-\omega_2$ can propagate over a long distance. Moreover, the directivity of this LF nonlinearly radiated signal can be even higher than the directivity of the HF primary waves [25]. Modeling of the parametric antenna operation in 3D disordered granular media has been recently reported [27] and applied for the interpretation of the experimental observations [28]. In this case, scattering due to contact disorder as well as velocity dispersion and absorption have been mainly studied.

For the following analysis, it is important that the difference frequency wave generated by mixing of two evanescent pump waves can be propagative and can carry information on the evanescent modes outside the region of their localization.

It should be pointed out that we are going to analyze weakly nonlinear waves, where the quadratic nonlinearity provides only a weak perturbation of the linear solution. In this case, an effect such as nonlinear supratransmission in the forbidden band gap by means of nonlinear modes [26] is not expected. However, energy transmission in the chain is possible even due to weak nonlinear effects if the interaction of the evanescent modes leads to the excitation of the propagative modes. In the following, we show that the LF signal, which might be experimentally transmitted in chains of beads, is sensitive to the transition from propagative to evanescent modes in the primary wave transport. The transition manifests itself by a strong decrease in the efficiency of the self-demodulation process.

Numerical computations are performed for both single frequency and wideband demodulated signals in order to include realistic experimental conditions: single frequency signals can be analyzed through a lock-in amplifier to access amplitude and phase, and wideband demodulated signals can be recorded in the temporal domain using an oscilloscope.

The influence of dispersion, absorption, and observation distance on the demodulated signal are analyzed for single frequency and wideband demodulated signals.

In Sec. II, the nonlinear equation of motion of the chain is first derived in the quadratic approximation. Then, using the dispersion relation in the chain for both propagative and evanescent modes, the solution for the LF wave demodulated from two pump frequencies is derived.

In Sec. III, the asymptotic analysis of this result is performed in different limiting cases, for propagative pump waves (strong and weak dispersive regimes), for evanescent waves, and in particular for pump frequencies in the vicinity of the cutoff frequency. The behavior of the nonlinear force and of the demodulated wave in the region of nonlinear interaction is also briefly analyzed.

Section IV presents the numerical treatment and the results for two kinds of HF pump wave signals, i.e., for two pump frequencies and for a Gaussian wave packet (a harmonic wave modulated in amplitude with a Gaussian function). The influence of dispersion for propagative HF pump waves on the demodulated wave amplitude and on its temporal profile is studied. Then, results on the influence of the transition from propagative to evanescent HF pump waves on the demodulated signal are presented. Finally, comparison of this transition with the transition from ballistics to diffusion in the HF pump wave propagation is discussed.

II. THEORY

A. Principle of the parametric emitting antenna

Due to the nonlinearity (or anharmonicity) of the lattice, the presence of an intense monochromatic HF wave at frequency ω creates a mean static nonlinear force. This phenomenon takes place, for instance, in the presence of thermal phonons, leading to dilatation in solids. When the monochromatic HF carrier wave is slowly modulated in amplitude, the nonlinear force is slowly accordingly modified. As a consequence, a LF wave is nonlinearly generated in the medium at the frequency of the modulation function.

It is possible to use different amplitude modulation profiles. Traditionally, the sinusoidal modulation of an harmonic carrier wave is described by $[1+m\cos(\omega_m t)]\cos(\omega t)$, where m is the modulation index, ω_m is the modulation frequency, and ω is the carrier frequency. The spectrum of such signal has three components $\omega, \omega-\omega_m$, and $\omega+\omega_m$. Another type of modulation can be obtained due to the beating phenomenon between two neighboring high frequencies ω_1 and ω_2. In this case, the spectrum of the primary signal is composed only of two frequencies ω_1 and ω_2, and the amplitude modulation of the total signal is a consequence of the relative phase variation between individual signals (being alternately in phase and out of phase).

In a medium with a quadratic elastic nonlinearity in the stress-strain relationship (corresponding to the cubic term in the potential energy–strain relationship), the superposition principle is no longer applicable, and waves at different frequencies can interact. This is commonly denoted as the frequency mixing phenomenon.

For two emitted neighboring HF waves ω_1 and ω_2 $(\omega_1 > \omega_2)$, the energy conservation principle ensures that frequencies $\omega_1+\omega_2$, $2\omega_1$, $2\omega_2$, 0, and $\omega_1-\omega_2$, which is a LF wave (if $|\omega_1-\omega_2| \ll \omega_1, \omega_2$), are generated. As the attenuation

increases with increasing frequency, only the LF component can propagate remotely and can be recorded. Thus, the primary emitted HF signal composed of ω_1 and ω_2 is nonlinearly self-demodulated into a signal at the frequency $\Omega = \omega_1 - \omega_2$.

Another possible regime of LF wave generation by the so-called parametric antenna [25] is the pulsed mode, where a finite length HF primary wave packet is emitted first. For simplicity of analytical development, and also to avoid the side lobes in the spectra of primary signals, Gaussian modulation functions of the carrier wave are considered in the following. The dependence of the mechanical displacement in the primary wave on time and the associated spectrum can be modeled by

$$U(t) = A\cos(\omega_0 t)e^{-t^2/2\tau_m^2}, \tag{1}$$

$$\tilde{U}(\omega) = A\tau_m\sqrt{\frac{\pi}{2}}\left(e^{-(\omega+\omega_0)^2(\tau_m^2/2)} + e^{-(\omega-\omega_0)^2(\tau_m^2/2)}\right), \tag{2}$$

where τ_m is the characteristic modulation time of the initial wave packet and ω_0 the central frequency of this wave packet. In this case, the frequency mixing takes place between all the frequency pairs of the Gaussian spectrum. Due to this, the solution $U_\Omega^{\text{Gauss}}(n,t,\omega_0,\tau_m)$ (where n is the space coordinate) for the demodulation of the Gaussian HF wave packet is related to the solution $U_\Omega(n,t,\omega_0,\Omega)$ describing the difference frequency $\Omega=\omega_1-\omega_2$ excitation in the case of two waves mixing. The following integration should be performed:

$$U_\Omega^{\text{Gauss}}(n,t,\omega_0,\tau_m) = \int_{-\infty}^{+\infty} U_\Omega(n,t,\omega_0,\Omega)e^{-\Omega^2\tau_m^2}d\Omega, \tag{3}$$

where $\omega_0=\omega_1$ and $\omega_0-\Omega=\omega_2$ and where $e^{-\Omega^2\tau_m^2}$ is proportional to the frequency spectrum of the pump intensity envelope. In the analysis section of this paper, the demodulated displacement $U_\Omega(n,t,\omega_0,\Omega)$ will be expressed with the help of a spectral transfer function $G(\omega_0,\Omega)$. Consequently, any change in the $G(\omega_0,\Omega)$ dependence on Ω will result in a modification of the shape of the demodulated temporal profile $U_\Omega^{\text{Gauss}}(n,t,\omega_0,\tau_m)$.

B. Equation of motion in the quadratic approximation

The considered problem is the elastic wave propagation in a semi-infinite 1D chain of identical spheres, as illustrated in Fig. 1. In the following, we will always consider the processes at the time scales which are much longer than the acoustic wave travel time along a bead diameter (i.e., less than 10^{-6} s for glass beads of diameter $a=2$ mm). The phenomena under investigation can be considered as quasistatic for the deformation of an individual bead; however, it does not imply that the wavelength of the elastic wave in the chain is large compared to the bead radius $a/2$ (because the sound velocity in the chain is much lower than the sound velocity in the bead material), and the discrete character of the chain will be always considered. As the elastic deformations are concentrated in the neighborhood of the contact location between two beads, it is possible to model the 1D granular chain as a chain of pointlike masses $m=\pi a^3\rho/6$ (where ρ is the bead material density) interacting by nonlinear springs with a Hertzian force-displacement law [14,15]

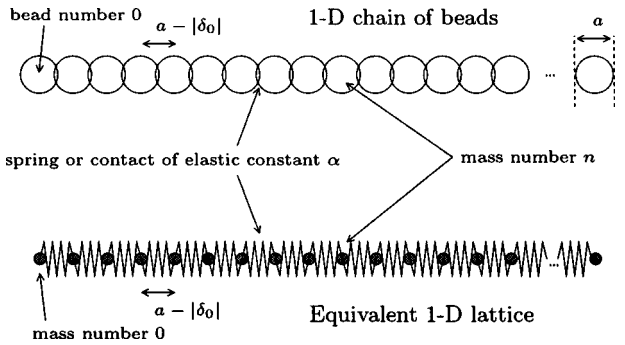

FIG. 1. Problem under consideration.

$$F_0 + F_d \propto (|\delta_0| + \delta_d)^{3/2}, \tag{4}$$

where F_0 is the static applied force on the chain, F_d is a small dynamic superimposed force, δ_0 is the static deviation of the interbead distance from a (a characteristic of the unloaded chain with $F_0=0$, $F_d=0$) and δ_d ($|\delta_d| \ll |\delta_0|$) is the perturbation due to the acoustic wave. Considering the case $F_0 \gg F_d$, the relation (4) can be expanded in a power series:

$$F_0 + F_d \propto |\delta_0|^{3/2} + \frac{3}{2}|\delta_0|^{1/2}\delta_d + \frac{3}{8}|\delta_0|^{-1/2}\delta_d^2 + \cdots. \tag{5}$$

The first nonlinear term of this expansion contains δ_d^2, which is quadratic. This expansion of the force-strain relationship between two beads can be also derived from a potential energy–displacement relation for the whole chain or equivalent 1D lattice (Fig. 1):

$$E_p = E_{p0} + \frac{\alpha}{2!}\sum_n [U(n) - U(n+1)]^2 + \frac{\beta}{3!}\sum_n [U(n) - U(n+1)]^3 + \cdots. \tag{6}$$

Here $U(n)$ denotes the displacement of the mass (or bead) number n. The cubic term in Eq. (6) corresponds to the quadratic nonlinearity of Eq. (5), α is the linear elastic constant of a contact, and β is the nonlinear quadratic parameter of the same contact. From this nonlinear relation, it is possible to deduce the following second order nonlinear equation of motion in discrete coordinates for each mass:

$$\begin{aligned} m\frac{\partial^2 U(n)}{\partial t^2} &= F(n) \\ &= -\frac{\partial E_p}{\partial U(n)} \\ &= \alpha[U(n+1) - 2U(n) + U(n-1)] \\ &\quad - \frac{\beta}{2}[U(n+1) - 2U(n) + U(n-1)] \\ &\quad \times [U(n+1) - U(n-1)]. \end{aligned} \tag{7}$$

The solutions of this nonlinear equation of motion for the self-demodulation process will be found via the usual successive approximation method [25].

C. Dispersion relation for the acoustic waves in the chain

First, we recall the linear properties of such a system, in particular the dispersion relation. These linear properties of elastic wave propagation in unidimensional lattices of identical masses and springs have been extensively studied [24]. The dispersion relation is obtained from the following linear equation of motion of the chain [the linear part of Eq. (7)]:

$$m\frac{\partial^2 U(n)}{\partial t^2} - \alpha[U(n+1) - 2U(n) + U(n-1)] = 0. \quad (8)$$

Eigenmodes of the infinite chain are derived in the form of waves $U(n)=\tilde{A}(\omega)e^{i\omega t-ikan}$, where ω is the angular frequency, $\tilde{A}(\omega)$ is the spectral amplitude, and k is the complex wave number. Substituting the last form of $U(n)$ into Eq. (8), the following well-known dispersion relation is obtained:

$$\omega^2 = \frac{4\alpha}{m}\sin^2\left(\frac{ka}{2}\right). \quad (9)$$

Introducing the notation $\omega_c=2\sqrt{\alpha/m}$ for the cutoff frequency, i.e., the maximum frequency of propagating waves, and $k_c=\pi/a$ for the maximum (real) wave number of propagating waves, it is possible to rewrite the relation (9) in the following form:

$$\sin^2\left(\frac{\pi}{2}\frac{k}{k_c}\right) = \left(\frac{\omega}{\omega_c}\right)^2. \quad (10)$$

Purely real solutions for the wave number k exist only if $|\omega|\leqslant\omega_c$. In this case, the dispersion relation is

$$\frac{\pi}{2}\frac{k}{k_c} = \pm\arcsin\left(\frac{\omega}{\omega_c}\right), \quad (11)$$

where the sign "+" corresponds to the waves propagating to the right (positive direction) and the sign "−" corresponds to the waves propagating to the left (negative direction). Considering only the waves propagating to the right, the following dispersion relation is obtained:

$$k = \frac{2}{\pi}k_c\arcsin\left(\frac{\omega}{\omega_c}\right) \quad \text{for} \quad -\omega_c\leqslant\omega\leqslant\omega_c. \quad (12)$$

If $|\omega|>\omega_c$, Eq. (10) has no purely real solution. It is necessary to consider the wave number k of the form $k=k'+ik''$ where k' and k'' are real. Then, from Eq. (10), it is possible to derive an expression for the evanescent wave number of the form

$$k = k_c\mathrm{sgn}(\omega) - i\frac{2}{\pi}k_c\,\mathrm{arcosh}\left(\frac{|\omega|}{\omega_c}\right) \quad \text{for} \quad |\omega|>\omega_c. \quad (13)$$

Note that Eq. (13) describes the dispersion of the evanescent modes that are attenuated in the positive direction (i.e., with increasing n). These are the modes for which the acoustic waves propagating in the positive direction are transformed above the critical frequency. The complete description of the wave dispersion relation of the chain is given by the combination of Eq. (12) and Eq. (13).

D. Solution for the self-demodulated wave

A parametric antenna emits low frequency signals (demodulated signals) due to the nonlinear rectification of powerful amplitude-modulated high frequency waves (primary waves) that are first radiated in the medium. Thus, there exists in the region of nonlinear excitation a large difference in amplitude between primary and demodulated waves. Using the method of successive approximations, i.e., considering that in the region of interaction, primary waves are much higher in amplitude than the nonlinearly demodulated waves, the equation of the first approximation for the HF primary waves is equivalent to Eq. (8), with the notation $U\equiv U_\omega$ to denote the displacement associated with the powerful primary waves. To describe the medium excitation by two high frequency waves we use the following boundary condition for the mass number 0 located at the boundary of the considered semi-infinite chain (Fig. 1):

$$U_\omega(n=0,t) = \mathrm{Re}[A_{\omega_1}(0)e^{i\omega_1 t} + A_{\omega_2}(0)e^{i\omega_2 t}]. \quad (14)$$

Here $A_{\omega_1}(0)$ and $A_{\omega_2}(0)$ are the complex amplitudes of the waves at frequencies ω_1 and ω_2 at the boundary $n=0$. The solution of Eq. (8) satisfying this boundary condition and the condition of radiation in the positive direction is

$$U_\omega(n,t) = \mathrm{Re}[A_{\omega_1}(0)e^{i\omega_1 t-ik(\omega_1)an} + A_{\omega_2}(0)e^{i\omega_2 t-ik(\omega_2)an}], \quad (15)$$

where $k(\omega)$ is the dispersion relation described by Eq. (12) and Eq. (13).

Due to the beating phenomenon between ω_1 and ω_2, the total signal is equivalent to an amplitude-modulated HF signal.

The demodulated LF displacement U_Ω is found with the equation of the second order approximation

$$\begin{aligned} m\frac{\partial^2 U_\Omega(n)}{\partial t^2} - \alpha[U_\Omega(n+1) - 2U_\Omega(n) + U_\Omega(n-1)] \\ = -\frac{\beta}{2}[U_\omega(n+1) - 2U_\omega(n) + U_\omega(n-1)] \\ \times[U_\omega(n+1) - U_\omega(n-1)], \end{aligned} \quad (16)$$

where the solution for U_ω is substituted in the right hand side of Eq. (7), while the contribution of U_Ω to the nonlinear terms is neglected. Retaining only the terms at frequency $\Omega=\omega_1-\omega_2$, it is possible to rewrite the right hand side of Eq. (16) as

$$2\beta\,\mathrm{Im}\left\{A_{\omega_1}(0)A^*_{\omega_2}(0)e^{i\Omega t-i(k_1-k_2^*)an}\left[\cos\left(\frac{k_1+k_2^*}{2}a\right)-\cos\left(\frac{k_1-k_2^*}{2}a\right)\right]\sin\left(\frac{k_1-k_2^*}{2}a\right)\right\}, \tag{17}$$

where $k_2=k(\omega_2)$, $k_1=k(\omega_1)$, and k_2^* denotes the complex conjugate of k_2. The general solution of Eq. (16) is the sum of the general solution of the homogeneous equation for waves of frequency Ω propagating in the positive direction and of a particular solution of the inhomogeneous equation

$$U_\Omega(n,t,\omega_1,\omega_2)=\mathrm{Im}[\underline{U}_\Omega(n,\omega_1,\omega_2)e^{i\Omega t}],$$

$$\underline{U}_\Omega(n,\omega_1,\omega_2)=C_1e^{-ik(\Omega)an}+C_2e^{-i\Delta k\ an},$$

$$C_2=\frac{\beta\,A_{\omega_1}(0)A^*_{\omega_2}(0)\left[\cos\left(\frac{k_1+k_2^*}{2}a\right)-\cos\left(\frac{k_1-k_2^*}{2}a\right)\right]\sin\left(\frac{k_1-k_2^*}{2}a\right)}{2\alpha\left[\sin^2\left(\frac{\Delta k}{2}a\right)-\frac{\Omega^2}{\omega_c^2}\right]}. \tag{18}$$

Here $\Delta k=k_2^*-k_1$, and C_1 and C_2 are two constants. Assuming the absence of the LF motion at the boundary ($n=0$), we get $C_1=-C_2$. The solution for the displacement in the demodulated wave takes the final form

$$U_\Omega(n,t,\omega_1,\omega_2)=\mathrm{Im}\left(\frac{\beta A_{\omega_1}(0)A^*_{\omega_2}(0)\left[\cos\left(\frac{k_1+k_2^*}{2}a\right)-\cos\left(\frac{k_1-k_2^*}{2}a\right)\right]\sin\left(\frac{k_1-k_2^*}{2}a\right)}{2\alpha\left[\frac{\Omega^2}{\omega_c^2}-\sin^2\left(\frac{\Delta k}{2}a\right)\right]}[1-e^{i[k(\Omega)-\Delta k]an}]e^{i\Omega t-ik(\Omega)an}\right). \tag{19}$$

III. ANALYSIS

In this section, the theoretical result (19) is analyzed for several limiting cases, including propagative pump waves and evanescent pump waves. First, the nonlinear force responsible for the self-demodulation process is simplified. This allows us to understand the basic properties of this parametric antenna operation. Second, the analysis of the displacement wave demodulated from the propagative pump waves is done out of the region of the nonlinear force action. Section III B 2 contains the qualitative analysis of the demodulated signal behavior inside the region of the nonlinear sources associated with propagative pump waves. Finally, the analysis of the displacement wave demodulated from evanescent pump waves is carried out. The following results allow us to explain the main physical features of the numerical results presented in Sec. IV.

A. Analysis of the nonlinear force

According to Eq. (7), the expression of the nonlinear force, quadratic in HF displacement, acting on the bead (or mass) number n is written

$$F_{\mathrm{NL}}(n)=-\frac{\beta}{2}[U(n+1)-2U(n)+U(n-1)]\times[U(n+1)-U(n-1)]. \tag{20}$$

The expression (15) of the displacement of the bead n, solution of the linear propagation equation (8) in the case of two excitation frequencies ω_1 and ω_2, is substituted in the expression (20). Retaining only the terms with the difference frequency $\Omega=\omega_2-\omega_1$, the nonlinear force (20) can be rewritten like the expression (17). When ω_1 tends to ω_2 ($\Omega=\omega_2-\omega_1$ tends to 0), this force is simplified in the form

$$F_{\mathrm{NL}}\simeq-2\beta\,\mathrm{Re}\{A_{\omega_1}(0)A^*_{\omega_2}(0)e^{i\Omega t}\}e^{-2|k''(\omega)|an}\times\{\cos[k'(\omega)a]-\cosh[|k''(\omega)|a]\}\sinh[|k''(\omega)|a], \tag{21}$$

where $k'(\omega)\simeq k'(\omega_1)\simeq k'(\omega_2)$ and $k''(\omega)\simeq k''(\omega_1)\simeq k''(\omega_2)$ are, respectively, the real and imaginary parts of the pump wave number for the high frequency $\omega\simeq\omega_1\simeq\omega_2$. In the low frequency limit $\omega\ll\omega_c$ and for weak attenuation $|k''|/|k'|\ll1$, a simpler form of the nonlinear force, responsible for the self-demodulation process, appears:

$$F_{\mathrm{NL}}\simeq\frac{a\beta}{\ell_a(\omega)}\frac{\omega^2}{\omega_c^2}\mathrm{Re}\{A_{\omega_1}(0)A^*_{\omega_2}(0)e^{i\Omega t}\}e^{-an/\ell_a(\omega)}. \tag{22}$$

This nonlinear force is proportional to the coefficient of quadratic nonlinearity β, and is proportional to the inverse of the characteristic attenuation length of the HF acoustic intensity $\ell_a(\omega)\equiv(2|k''(\omega)|)^{-1}$. This force decreases like $e^{-an/\ell_a(\omega)}$ with increasing distance.

If the phases of the pump waves at $n=0$ are equal, the complex amplitudes $A_{\omega_1}(0)$ and $A^*_{\omega_2}(0)$ are real, and the notation A_1,A_2 can be used. Further, if $A_1=A_2=A$, the term A_1A_2 is equal to A^2 where A is the excitation amplitude of

both waves at frequency ω_1 and ω_2. In this case, the nonlinear force (22) varies like the squared pump wave amplitude A^2. The low frequency regime ($\omega \ll \omega_c$) described by Eq. (22) is identical to the regime of 1D (plane-wave) parametric antenna in homogeneous media [25].

B. Analysis of the LF demodulated signal

The analysis of the demodulated displacement $U(n)$ at the low frequency Ω, obtained in the form of Eq. (19), is done first for propagative pump waves and second for evanescent pump waves. Outside the excitation region, i.e., when the term $e^{-an/\ell_a(\omega)}$ of Eq. (19) or Eq. (22) tends to 0 (the pump waves are sufficiently attenuated), the nonlinear force becomes negligible. The LF demodulated wave is then entirely generated, and propagates freely in the medium. In this case, the demodulated wave $\underline{U}_\Omega(n)$ is equal to a function $G(\omega_1,\omega_2)$ multiplied with a phase term $(1-e^{ik(\Omega)an-i\Delta kan})e^{-ik(\Omega)an} \simeq e^{-ik(\Omega)an}$ which describes its propagation in the dispersive medium. This function $G(\omega_1,\omega_2)$ represents a spectral transfer function describing the nonlinear process of difference frequency excitation by the self-demodulation process. It gives the opportunity, together with the phase term, to find the amplitude and the phase of the demodulated signal at frequency $\Omega=\omega_1-\omega_2$ from the knowledge of the pump waves emitted at frequencies ω_1 and ω_2. Importantly, $G(\omega_0,\Omega)=G(\omega_1=\omega_0,\omega_2=\omega_0-\Omega)$ can also be applied for the analysis of the case when a HF wave packet is used for the pump. Then, in accordance with Eq. (3) and the definition of $U_\Omega(n,t,\omega_1=\omega_0,\omega_2=\omega_0-\Omega)$ in Eq. (19), out of the antenna body ($n \gg 1$),

$$U_\Omega(n \gg 1,t,\omega_0,\tau_m) = \mathrm{Im}\int_{-\infty}^{+\infty} G(\omega_0,\Omega)e^{-\Omega^2\tau_m^2}\exp\left[i\Omega\left(t-\frac{k(\Omega)}{\Omega}an\right)\right]d\Omega. \tag{23}$$

Consequently, the product $2\pi G(\omega_0,\Omega)e^{-\Omega^2\tau_m^2}$ provides the spectrum of the demodulated wave in the accompanying system of coordinates when $n \gg 1$. In other words, the spectrum of the demodulated signal might be obtained by multiplication of the spectrum of the intensity envelope of the HF wave $e^{-\Omega^2\tau_m^2}$ by the function $G(\omega_0,\Omega)$. This is the reason to call $G(\omega_0,\Omega)$ the spectral transfer function. In order to understand the LF generation dynamics in the region of the nonlinear sources and particularly the role of the velocity dispersion, the whole phase term $(1-e^{ik(\Omega)an-i\Delta kan})e^{-ik(\Omega)an}$ will also be analyzed in the following.

For the analysis of the self-demodulation process, the pump wave frequencies ω and the associated wave numbers are respectively normalized to the cutoff frequency ω_c and to the factor $(2/\pi)k_c$. The main advantage of such a normalization is that both the phase velocity c_ϕ and the group velocity c_g are equal to 1 when the frequency ω tends to 0.

When these normalizations are done, the transfer function of the self-demodulation process takes the following general form:

$$G(\omega_1,\omega_2) = \frac{\beta}{2\alpha}A^2\frac{[\cos(k_1-k_2^*)-\cos(k_1+k_2^*)]}{\Omega^2-\sin^2(k_1-k_2^*)}\sin(k_1-k_2^*). \tag{24}$$

In the following, the notation $\omega_1=\omega, \omega_2=\omega-\Omega$ with $\Omega>0$ is used.

1. Case of propagative pump waves

In the case of propagative pump waves, in contrast to the evanescent ones for which a further exact development of the transfer function G is possible, it is necessary to consider that $|\Omega| \ll |\omega|$.

The relation $0<\Omega \ll \omega \leqslant 1$ is then satisfied. Taking into account these equalities and inequalities, each term of the transfer function (24) can be simplified.

Considering that the attenuation of the propagative waves is sufficiently weak to allow their propagation, i.e., the modulus of the imaginary part of the wave number $|k''(\omega)| \ll 1$, and neglecting the dispersion of attenuation $[|k''(\omega)| \simeq |k''(\omega-\Omega)|]$, the imaginary part of the difference $(k_1-k_2^*)$ is written as $2i|k''(\omega)|$. Using the Taylor expansion of the dispersion relationship at the first order, valid for $|\Omega| \ll |(\partial k'/\partial\omega)/(\partial^2 k'/\partial\omega^2)|$, the real term $(k_1'-k_2')$ is approximated by $k_1'-k_2' \simeq \Omega(\partial k'/\partial\omega)(\omega) \ll 1$. In this case,

$$\sin(k_1-k_2^*) \simeq \Omega\frac{\partial k'}{\partial\omega}(\omega)+2i|k''(\omega)|, \tag{25}$$

$$\cos(k_1-k_2^*) \simeq 1 \tag{26}$$

at the first order in $\Omega(\partial k'/\partial\omega)(\omega)$ and in $|k''(\omega)|$. With the same approximations,

$$\cos(k_1+k_2^*) \simeq 1-2\omega^2+2\omega\sqrt{1-\omega^2}\Omega\frac{\partial k'}{\partial\omega}(\omega). \tag{27}$$

Substituting the simplified terms (26) and (27) in the expression of the transfer function (24), and using $(\partial k'/\partial\omega)\omega = c_g^{-1}(\omega)=(1-\omega^2)^{-1/2}$, where $c_g(\omega)$ denotes the group velocity, a new expression for the transfer function G is obtained:

$$G(\omega,\Omega) \simeq \frac{\beta}{\alpha}A^2\omega^2\frac{\Omega/c_g(\omega)+2i|k''(\omega)|}{\{[\Omega/c_g(\omega)]+2i|k''(\omega)|\}^2-\Omega^2}. \tag{28}$$

Using the notation $\ell_a(\omega)=1/2|k''(\omega)|$ for the attenuation length of the acoustic pump intensity, and considering that for a qualitative analysis of the behavior of $G, 1+c_g(\omega)$ is of the same order as $1(0 \leqslant c_g(\omega) \leqslant 1)$, the expression (28) is simplified to the form

$$G(\omega,\Omega) \sim \frac{\beta}{\alpha}A^2\omega^2\ell_a(\omega)\frac{1}{p+i} \tag{29}$$

where $p=p'[1-c_g(\omega)]=\ell_a(\omega)k(\Omega)[c_\phi(\Omega)/c_g(\omega)][1-c_g(\omega)]$ is a nondimensional parameter. With $\Omega \ll \omega \leqslant 1$, the relation $c_\phi(\Omega) \simeq c_\phi(0)=1$ is satisfied, and the parameter p can be rewritten as

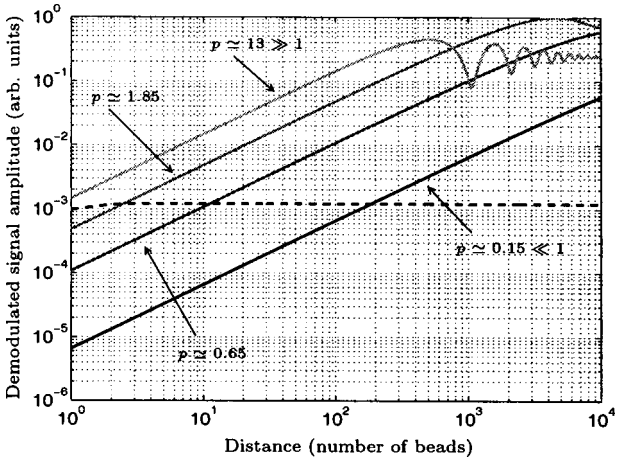

FIG. 2. Demodulated displacement amplitude as a function of the observation distance (expressed in number of beads n) for four different values of the nondimensional parameter p. For comparison, the amplitude of the demodulated signal from evanescent pump waves is plotted as a dashed line.

$$p \simeq \ell_a(\omega) k(\Omega) \frac{c_\phi(\Omega) - c_g(\omega)}{c_g(\omega)}. \tag{30}$$

In this expression, $\ell_a(\omega)/c_g(\omega)$ represents the time taken by the HF pump wave packet to travel along its characteristic attenuation region. The factor $[\ell_a(\omega)/c_g(\omega)][c_\phi(\Omega) - c_g(\omega)]$ represents the characteristic spatial separation between the HF pump wave packet and the demodulated signal at the scale $\ell_a(\omega)$, i.e., at the limit of the nonlinear interaction region. So the parameter p is proportional to this distance measured in LF acoustic wavelengths.

First limiting case. When $p \ll 1$, this spatial separation is small compared to the wavelength $\lambda(\Omega)$ of the demodulated signal, and the transfer function takes the following form:

$$G(\omega,\Omega) \sim -i \frac{\beta}{\alpha} A^2 \omega^2 \ell_a(\omega). \tag{31}$$

In this case, the amplitude variation of the demodulated signal as a function of the pump frequency is controlled by the pump wave attenuation [parameter $\omega^2 \ell_a(\omega)$]. The velocity dispersion does not play an important role, either due to the small antenna length, or due to the small difference between the velocities $c_g(\omega)$ and $c_\phi(\Omega)$, in producing a sufficient spatial separation between the HF wave packet and the LF demodulated signal at the end of the interaction region. In this limiting case, the function G being independent of the variable Ω, the demodulated displacement temporal profile (in the case of the demodulation of a wave packet) remains qualitatively unchanged compared to the initial modulation function of the pump signal [$|U_\Omega(n,t,\omega_0,\Omega)|$ is independent of Ω in Eq. (3)].

For an attenuation length of the form $\ell_a(\omega) \sim 1/\omega$, as is considered later, the transfer function $G(\omega,\Omega)$ increases linearly with the pump frequency ω. This first limiting case corresponds to the $p \simeq 0.15$ curve in Fig. 2 of the numerical results section, and to curve $p \simeq 0.13$ of Fig. 3.

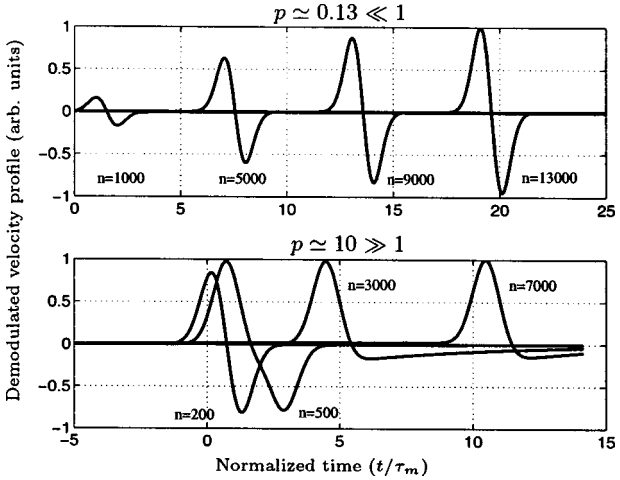

FIG. 3. Evolution of the demodulated temporal velocity profile with the observation distance in two limiting cases $p \ll 1$ and $p \gg 1$.

Second limiting case. When $p \gg 1$, this spatial separation is large compared to the wavelength $\lambda(\Omega)$ of the demodulated wave, and the transfer function takes the following form:

$$G(\omega,\Omega) \sim \frac{\beta}{\alpha} A^2 \frac{\omega^2 \sqrt{1-\omega^2}}{\Omega(1-\sqrt{1-\omega^2})} \tag{32}$$

where $c_g(\omega) = \sqrt{1-\omega^2}$. This development is valid only for $(1-\omega) \gg \Omega$, which ensures the validity of the Taylor development of the dispersion relation carried out previously with the small parameter Ω. It is already possible to say that in the case of an excitation with a HF pump wave packet [as considered in Eq. (3)], the demodulated temporal profile will be integrated due to the presence of the factor Ω in the denominator of expression (32). Two limiting cases (giving the same form for G) can be identified in the expression (32), the case of small velocity dispersion where $\omega \ll 1$ [in this case $c_g(\omega) \simeq c_\phi(\Omega) \simeq 1$] and the case of strong velocity dispersion where ω is near 1 [$c_g(\omega) \ll c_\phi(\Omega)$] in the limit, however, where $1-\omega \gg \Omega$.

When $\omega \ll 1$, the function G has the form

$$G(\omega,\Omega) \sim \frac{\beta}{\alpha} A^2 \frac{1}{\Omega}. \tag{33}$$

The conditions $p \gg 1$ and $\omega \ll 1$ mean that the length scale where nonlinear interaction takes place, $\ell_a(\omega)$, is large compared to the demodulated signal wavelength $\lambda(\Omega)$, i.e., although the velocity difference is small, the interaction region is sufficiently long for the spatial separation between HF nonlinear sources and the demodulated wave to be significant. In this case, the function $G(\omega,\Omega)$ is independent of the pump frequency ω, meaning that out of the antenna body, the demodulated signal amplitude does not depend on ω.

When ω tends to 1 (still with $1-\omega \gg \Omega$), the function G has the following form:

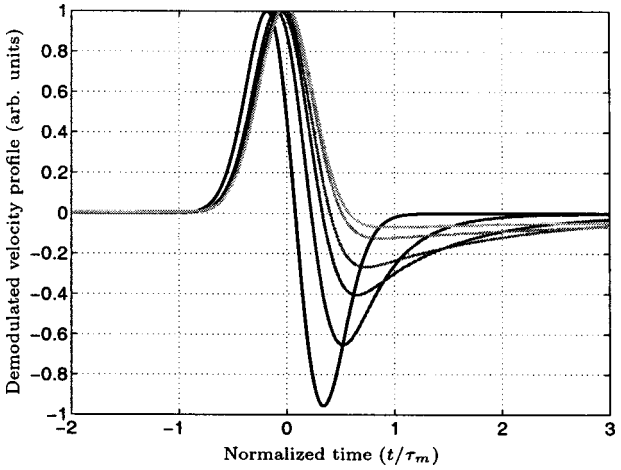

FIG. 4. Transition in the velocity profile, demodulated from propagative pump waves, associated with the sound dispersion. The parameter p is, from the darkest to the lightest line, 0.16, 0.73, 1.6, 2.76, 6.6, 12.2, respectively, $C=2\times10^{-7}$, and $\Omega\simeq1.7\times10^{-3}$.

$$G(\omega,\Omega)\simeq\frac{\beta}{\alpha}A^2\frac{\sqrt{1-\omega^2}}{\Omega}. \tag{34}$$

The velocity difference between $c_g(\omega)$ and $c_\phi(\Omega)$ is significant, which ensures a strong influence of the velocity dispersion on the demodulated signal. The factor $\sqrt{1-\omega^2}$ that appears in the denominator of expression (34) describes the decrease of the demodulated wave amplitude when ω approaches the cutoff frequency 1.

In these two last limiting cases, the dependence of G on Ω is identical; the velocity dispersion influence is significant and manifests itself by a temporal integration of the demodulated LF signal. This is illustrated in Sec. IV, by the profile $n=7000$, $p\simeq10$ in Fig. 3. Transition between the limiting cases $p\ll1$ and $p\gg1$ is shown in Fig. 4.

Limiting case ω tends to 1. The interest in analyzing this limiting case, where the condition $\Omega\gg1-\omega$ is satisfied (ω is in the vicinity of the cutoff frequency 1), is to check the correspondence between the high frequency limit of the propagative zone and the low frequency limit of the evanescent zone (case studied later in Sec. III B 3).

When $\Omega\gg1-\omega$, the Taylor expansion of the term $k_1'-k_2'$ cannot be done with the help of the small parameter Ω, but should be derived with the $1-\omega$ small parameter:

$$k_1'-k_2'\simeq-\sqrt{2\Omega}+\sqrt{2(1-\omega)}\simeq-\sqrt{2\Omega}, \tag{35}$$

and the following terms, which appear in the general form of the transfer function (24), have the forms:

$$\sin(k_1-k_2^*)\simeq-\sqrt{2\Omega}-2i|k''(\omega)|,$$

$$\cos(k_1-k_2^*)\simeq1-\frac{1}{2}[\sqrt{2\Omega}+2i|k''(\omega)|]^2,$$

$$\cos(k_1+k_2^*)\simeq-1+\Omega. \tag{36}$$

These expressions (36) are substituted in Eq. (24) to obtain a new expression for the transfer function G:

$$G(\omega,\Omega)\simeq\frac{\beta}{\alpha}A^2\frac{\sqrt{2\Omega}+2i|k''(\omega)|}{\Omega^2-\left[\sqrt{2\Omega}+2i|k''(\omega)|\right]^2}. \tag{37}$$

As $\Omega\ll1$, the term Ω^2 in the denominator of this expression is always negligible compared to Ω. The notation $2|k''(\omega)|=1/\ell_a(\omega)$ is reintroduced and G is simplified:

$$G(\omega,\Omega)\simeq-\frac{\beta}{\alpha}A^2\frac{1}{\sqrt{2\Omega}+2i|k''(\omega)|}. \tag{38}$$

By introducing the nondimensional parameter $P=\sqrt{\Omega/2}\ell_a(\omega)$, the function G is rewritten as

$$G(\omega,\Omega)\simeq-\frac{\beta}{2\alpha}A^2\ell_a(\omega)\frac{1}{P+i}. \tag{39}$$

When the condition $1-\omega\gg\Omega$ holds, which was the case in the previous subsection, the characteristic pump frequency is $(\omega_1+\omega_2)/2=(\omega+\omega-\Omega)/2\simeq\omega$ when $\Omega\ll\omega$. Inversely, in the present analysis, the condition $1-\omega\ll\Omega$ implies that the characteristic pump frequency is now $(\omega_1+\omega_2)/2=(\omega+\omega-\Omega)/2=[2+2(1+\omega)-\Omega]/2\simeq1-\Omega/2$. In this limiting case $(1-\omega\ll\Omega)$, the parameter p used for the analysis of the previous case $1-\omega\gg\Omega$ can be rewritten as

$$p=\ell_a(\omega)\frac{\Omega}{c_\phi(\Omega)}\frac{c_\phi(\Omega)-c_g(\omega)}{c_g(\omega)}\simeq\ell_a(\omega)\frac{\Omega}{c_g(1-\Omega/2)} \tag{40}$$

with $c_\phi(\Omega)\simeq1$ and $c_g(\omega)\simeq c_g(1-\Omega/2)\to0$. Finally, as $c_g(1-\Omega/2)\simeq\sqrt{1-(1-\Omega/2)^2}\simeq\sqrt{\Omega}$, the previous parameter p is equivalent to the new one P. The physical interpretations of these parameters are thus identical when taking into account the difference in the characteristic frequencies of HF waves in the considered situations.

When $P\ll1$, the phase mismatch between the nonlinear sources and the demodulated signal at the limit of the interaction region is weak, and the transfer function takes the form

$$G(\omega,\Omega)\simeq-i\frac{\beta}{2\alpha}A^2\ell_a(\omega). \tag{41}$$

This function is proportional to $\ell_a(\omega)$ and does not depend on Ω. This limiting case corresponds to the limit $p\ll1,1-\omega\gg\Omega$, the expression of Eq. (31).

When $P\gg1$, the phase mismatch between the nonlinear sources and the demodulated signal at the limit of the interaction region is large, and the transfer function has the form

$$G(\omega,\Omega)\simeq-\frac{\beta}{2\alpha}A^2\frac{1}{\sqrt{\Omega}}. \tag{42}$$

In this case, the factor $1/\sqrt{\Omega}$ ensures the partial integration (of the order of $1/2$) of a temporal profile, demodulated from a pump wave packet [a consequence of the substitution of this term in Eq. (3)]. From the comparison of Eq. (34) and Eq. (42) it can be concluded that when (for the fixed $\Omega\ll\omega$) the frequency ω approaches 1, the integration of the profile transforms into partial integration.

2. Behavior in the region of the nonlinear sources

The analysis of the result (19) in the region of the nonlinear sources, i.e., when $|e^{ik(\Omega)an-i\Delta kan}|$ is not small compared to 1, is justified for propagative pump waves. For evanescent pump waves, attenuated along a distance of several beads, the source region is so limited in space that the observation is too difficult to be realized in this region. The result (19) is the product of the phase term $(1-e^{ik(\Omega)an-i\Delta kan})e^{i\Omega t-ik(\Omega)an}$ and of the transfer function $G(\omega,\Omega)$ studied earlier for propagative pump waves. Thus, only the phase term should be analyzed. The term $e^{i\Omega t-ik(\Omega)an}$ describes the propagation of the demodulated LF wave in the chain. The term $1-e^{ik(\Omega)an-i\Delta kan}$ is thus to be analyzed. It is controlled by the behavior of the following phase Φ:

$$\Phi=[\Delta k-k(\Omega)]an. \tag{43}$$

In the limit where the attenuation of the pump waves is weak, the modulus of $e^{ik(\Omega)an-i\Delta kan}$ is close to 1. In the following analysis, the imaginary part of the propagative wave number is neglected and the wave numbers and frequencies are normalized [respectively to $(2/\pi)k_c$ and ω_c]. Moreover $\Delta k=k'(\omega_1)-k'(\omega_2)$ can be simplified if $k'(\omega_1=\omega+\Omega/2)$ and $k'(\omega_2=\omega-\Omega/2)$ are expanded in Taylor series (under the condition $1-\omega\gg\Omega$). In this case, $\Delta k\simeq\Omega/c_g(\omega)$ up to the third order in Ω.

The wave number $k(\Omega)$ is equal to $\Omega/c_\phi(\Omega)$, where $c_\phi(\Omega)$ is the phase velocity at low frequency Ω. This phase velocity is obtained from the dispersion relation (12), having the form $c_\phi(\Omega)=\Omega/\arcsin(\Omega)\simeq 1$ for $\Omega\ll 1$. The group velocity at high frequency is also derived from the dispersion relation (12) and is equal to $c_g(\omega)=c_\phi(0)\sqrt{1-\omega^2}$. Consequently, the phase (43) to be analyzed can be rewritten with normalized quantities:

$$\Phi=-2\Omega\left(1-\frac{1}{c_g(\omega)}\right)n. \tag{44}$$

If this phase is equal to $-2\pi\ell$ or $-(2\ell+1)\pi$ with $\ell\in\mathbb{N}$ the term $1-e^{ik(\Omega)an-i\Delta kan}$ of the result (19) has a minimum or a maximum, respectively. The pump frequencies for which a minimum is obtained satisfy the following relation:

$$\omega=\sqrt{1-\left(1-\frac{\pi\ell}{\Omega n}\right)^{-2}}. \tag{45}$$

The distances for which a minimum is obtained are

$$n=\frac{\pi\ell}{\Omega}[1-(1-\omega^2)^{-1/2}]^{-1}. \tag{46}$$

If the pump wave absorption is taken into account, the term $1-e^{ik(\Omega)an-i\Delta kan}$ of Eq. (19) has minima (or maxima) less pronounced because the modulus of $e^{ik(\Omega)an-i\Delta kan}$ is no longer equal to 1 but becomes smaller. Its behavior depends on the difference between the phase velocity of the LF demodulated wave $c_\phi(0)\simeq 1$ and the HF group velocity of the nonlinear sources $c_g(\omega)$. In the region of existence of the nonlinear sources, the occurrence of a succession of minima and maxima in the amplitude of the demodulated LF wave is thus a manifestation of an effect of velocity dispersion associated with the asynchronism between nonlinear sources and the demodulated wave. This behavior is clearly depicted as a function of the propagation distance in Fig. 2 and as a function of the pump frequency in Fig. 5.

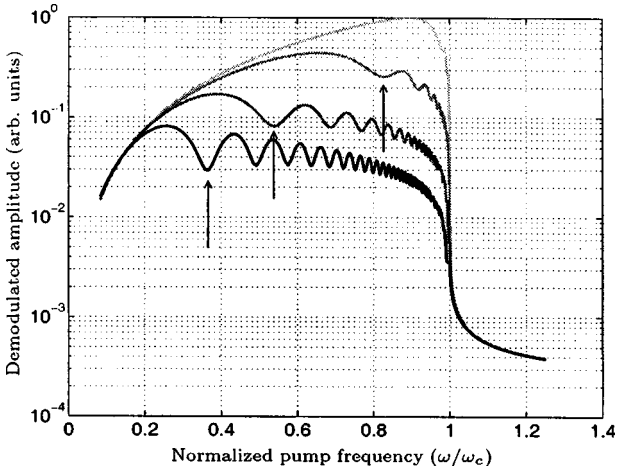

FIG. 5. Transition between the generation of the demodulated signal by propagative pump waves and by evanescent pump waves. The observation distance is fixed, $n=5000$, the attenuation constant is $C=5\ 10^{-7}$, and demodulated frequencies are respectively from the brightest to the black lines $\Omega\simeq 1.7\ 10^{-4}; 8.3\ 10^{-4}; 3.3\ 10^{-3}$ and $8.3\ 10^{-3}$.

3. Case of evanescent pump waves

The pump waves become evanescent when the pump frequency ω is higher than the cutoff frequency of the granular chain ω_c. They are localized near the high frequency emitter. Consequently, the demodulated signal is almost always registered out of the region of nonlinear interaction [the modulus of the term $e^{-i\Delta kan}$ of Eq. (19) is much less than 1].

For the analysis of the demodulation of evanescent pump waves, it is possible to start from the general expression of the transfer function (24). Frequencies and wave numbers are still normalized, respectively, to ω_c and $2k_c/\pi$. Considering $\omega_2=\omega$ and $\omega_1=\omega+\Omega$ with $\Omega>0$, and using the dispersion relation Eq. (13), the transfer function (24) can be rewritten as a function of ω and Ω:

$$G(\omega,\Omega)=-i\frac{\beta}{\alpha}A^2\frac{\omega(\omega+\Omega)\left[\omega\sqrt{(\omega+\Omega)^2-1}+(\omega+\Omega)\sqrt{\omega^2-1}\right]}{\Omega^2+\left[\omega\sqrt{(\omega+\Omega)^2-1}+(\omega+\Omega)\sqrt{\omega^2-1}\right]^2}. \tag{47}$$

Taking into account the fact that $\Omega\ll\omega$, and for pump frequencies sufficiently far from the cutoff frequency ($\omega-1\gg\Omega$), this expression becomes

$$G(\omega,\Omega)\simeq-i\frac{\beta}{\alpha}A^2\frac{\omega}{2\sqrt{\omega^2-1}}. \tag{48}$$

It is interesting to note that in this case, when ω becomes large compared to the cutoff frequency 1, the modulus $|G(\omega,\Omega)|\sim\beta A^2/\alpha 2$ is independent of the pump frequency ω and independent of the difference frequency Ω. The nonlin-

ear sources are localized on the very first beads due to their evanescent nature, which means that they can be considered (for $\omega^2 \gg 1$) as surface sources for the LF demodulated wave. As a consequence, no dispersion effect can influence the process of self-demodulation which ensures that no frequency dependence is observed.

Inversely, still considering that $\Omega \ll \omega$, but for pump frequencies in the vicinity of the cutoff frequency ($\omega - 1 \ll \Omega$), the transfer function is

$$G(\omega,\Omega) \simeq -i\frac{\beta}{\alpha}A^2\frac{\sqrt{2}}{\sqrt{\Omega}}. \tag{49}$$

The limit (48) shows that in the case of the demodulation of a pump wave packet, the demodulated temporal displacement will exhibit a profile identical to the intensity modulation function of this HF wave packet, due to the absence of dependence on Ω. In contrast, the limit (49) ensures that the temporal profile of the demodulated displacement is partially integrated due to the presence of the term $\sqrt{\Omega}$ in the denominator.

For the analysis of the demodulated signal from evanescent pump waves, the convention $\omega_2 = \omega$ and $\omega_1 = \omega + \Omega$ with $\Omega > 0$ has been used, but for the analysis of the demodulated signal from propagative pump waves it is the convention $\omega_1 = \omega$ and $\omega_2 = \omega - \Omega$ with $\Omega > 0$ which has been used. Comparison of the result (49) obtained in the evanescent limit $\omega \to 1, \omega > 1$ and of the result (42) obtained in the propagative limit $\omega \to 1, \omega < 1$, should thus be carried out by changing in one of the two cases Ω by $-\Omega$. This produces a factor $-i$ in the transfer function where $-\Omega$ is introduced [due to the term $(\Omega)^{-1/2}$ which occurs in these limiting cases], and the two results agree well. Continuity of $G(\omega,\Omega)$ across the transition from $\omega < 1$ to $\omega > 1$ is also confirmed by the numerical results taking into account the total expression (19) (see Fig. 5).

4. General qualitative analysis of the dependence of the demodulated signal on ω and Ω

The demodulated displacement is proportional in the general case to

$$\underline{U}_\Omega \sim \frac{F_{\mathrm{NL}}(n=0,\omega,\Omega)}{\Omega^2 - \sin^2(\Delta k)} \tag{50}$$

where F_{NL} is the nonlinear force acting in the demodulation process (the time dependence $e^{i\Omega t}$ is omitted). The denominator of "resonant" type is common for forced processes. In the limiting case $\omega \ll 1$ (the nondimensional parameter $p \ll 1$), characterized by a negligible role of the dispersion effects, the denominator describes synchronism effects and the net effect is proportional to the length of their accumulation, i.e., proportional to the length of the antenna $\ell_a(\omega)$:

$$\frac{1}{\Omega^2 - \sin^2(\Delta k)} \sim \ell_a(\omega)\lambda(\Omega). \tag{51}$$

In contrast, in the opposite limiting case $\omega \gg 1$, there are no effects of the signal accumulation just because the antenna is reduced to a single (first) nonlinear spring near the surface. In this limit,

$$\sin^2(\Delta k) \simeq -\sinh^2[2|k''(\omega)|] \sim e^{4|k''(\omega)|} \sim \omega^4 \tag{52}$$

strongly dominates in the resonant denominator and the conditions for the signal accumulation rapidly diminish with increasing ω.

However, in accordance with Eq. (50), not only the accumulation of the signal but also the magnitude of the forces should be compared in these two limiting cases. The nonlinear force acting on the bead number n is equal to the difference of the forces applied from different sides. From Eq. (7),

$$F_{\mathrm{NL}}(n) \sim [U_\omega(n+1) - U_\omega(n)]^2 - [U_\omega(n) - U_\omega(n-1)]^2. \tag{53}$$

In the low frequency limit ($\omega \ll 1$), each of the strains $[U_\omega(n+1) - U_\omega(n)]/a$ and $[U_\omega(n) - U_\omega(n-1)]/a$ is inversely proportional to the HF acoustic wavelength, that is, proportional to ω. The differences between the forces applied to the bead from different sides are controlled by HF wave absorption or by the difference in the high frequencies, that is, by Ω. As a result, in the limit $\omega \ll 1$,

$$F_{\mathrm{NL}} \sim \omega^2 \max\{k(\Omega), k''(\omega)\}.$$

In the case of a high quality antenna, $\ell_a(\omega) \gg \lambda(\Omega)$ [25], and

$$F_{\mathrm{NL}} \sim \omega^2 k(\Omega). \tag{54}$$

Consequently, from Eq. (50), Eq. (51) and Eq. (54),

$$\underline{U}_\Omega \sim \omega^2 \ell_a(\omega), \tag{55}$$

which is the classical result for the 1D parametric antenna in a homogeneous medium [25].

In the limit $\omega \gg 1$, the situation is different. The force F_{NL} in Eq. (53) is controlled by the displacement of the single lowest number bead. Formally,

$$F_{\mathrm{NL}}(n=0,\omega,\Omega) \sim -U_\omega^2(-1) \sim e^{4|k''(\omega)|} \sim \omega^4. \tag{56}$$

Thus, the localization of the force leading to the dependence $\sim\omega^4$ of the denominator is completely compensated by the increase of force amplitude ($\sim\omega^4$) described by Eq. (56). Consequently, in the regime $\omega \gg 1$, $\underline{U}_\Omega$ depends neither on Ω nor on ω.

This qualitative analysis confirms the result obtained earlier on the basis of the asymptotic expansions. In the intermediate frequency range $\omega \sim 1$ (or, in general, when the nondimensional parameters p and P are not small), the influence of the wave velocity dispersion on the spectral transfer function $G(\omega_0,\Omega)$ should be taken into account.

IV. NUMERICAL TREATMENT AND RESULTS

As previously, frequencies and wave numbers are normalized for numerical calculus and in the presentation of the results. The quantities that can be varied experimentally such as the pump frequency ω, the modulation frequency Ω, or the observation distance n (number of beads) are used in the following to vary the nondimensional parameters of the problem p and P, and to go from one previously analyzed

limiting case to another. The attenuation of the propagative pump waves is taken into account through an imaginary part of the wave number of the form $|k''(\omega)|=C\omega$ where C is a constant. This frequency dependence of the attenuation has been experimentally observed in three-dimensional granular media [13]. However, it is possible to introduce in this formalism any kind of function of the frequency to describe the attenuation, including, for instance, nonmonotonic functions for relaxation phenomena.

A. Influence of the observation distance

In order to understand the different regimes of the parametric antenna operation, it is interesting to plot the demodulated signal amplitude as a function of the observation distance, especially in the region of existence of the nonlinear sources.

1. Case of two pump frequencies

In the case of two neighboring pump frequencies ω_1 and ω_2 (the only demodulated frequency is thus $\Omega \ll \omega_1, \omega_2$), the demodulated signal amplitude is plotted as a function of the distance for different values of the nondimensional parameter p, on Fig. 2. In this simulation, $\Omega \simeq 8\times10^{-4}$, and $C=2\times10^{-7}$. As $\Omega \ll \omega_1, \omega_2$, it is possible to consider for the discussion that $\omega_1 \simeq \omega_2 \simeq \omega$. In Fig. 2, four curves are plotted in continuous lines and correspond to four values of the nondimensional parameter $p \simeq 0.15, 0.65, 1.85, 13$ obtained by varying the pump frequency respectively, as $\omega \simeq 8\times10^{-2}, 3\times10^{-1}, 6\times10^{-1}, 0.98$. For these pump frequencies the attenuation length of the pump intensity (characteristic length of the parametric antenna) is, respectively, in terms of the number of beads, $\ell_a(\omega)/a \simeq 3.2\times10^4, 0.8\times10^4, 0.4\times10^4, 0.23\times10^4$. The observation of the demodulated signal is thus mainly realized in the region of nonlinear interaction between the pump waves.

For $p \ll 1$, the demodulated amplitude is proportional to the distance $|1-e^{ik(\Omega)an-i\Delta kan}| \equiv |1-e^{\xi n}| \simeq |1-1-\xi n| \simeq |\xi n|$ (in the limit $|\xi| n \ll 1$) (see the curve $p \simeq 0.15$ of Fig. 2). For $p \gg 1$, the same dependence is observed along a distance of several hundred beads, but a saturation phenomenon appears. The demodulated amplitude reaches then a maximum value and begins to oscillate between local minima and maxima (see the curve $p \simeq 13$ of Fig. 2). This behavior has been discussed in Sec. III B 2, and is associated with the velocity difference between the nonlinear sources that propagate at the velocity $0 \leqslant c_g(\omega) \leqslant 1$ and the demodulated wave that propagates at the velocity $c_\phi(\Omega) \simeq 1$. In accordance with Eq. (46) obtained from the analysis of the phase term of the demodulated displacement (19), the first minimum for $\ell = -1, \Omega \simeq 8\times10^{-4}$, and $\omega \simeq 0.98$ should appear at the distance $n \simeq 1100$, and the following minima at multiple integer distances. This behavior is well observed for $p \simeq 13$ in Fig. 2.

For comparison, the demodulated signal amplitude from evanescent pump waves ($\omega \simeq 1.083$) is plotted as a dashed line on the same Fig. 2. This amplitude is constant, starting from several beads, i.e., out of the region of existence of the pump waves.

2. Case of a Gaussian pump wave packet

In the case of the demodulation of a pump wave packet with a Gaussian spectrum (or equivalently modulated by a Gaussian temporal function), the manifestation of the effects previously mentioned is different. The velocity dispersion does not produce minima and maxima in the demodulated displacement amplitude, but gives an amplitude saturation and a widening of the temporal profile of this signal. This behavior is directly linked to the fact that the nonlinear sources propagate more slowly than the demodulated signal they generate $[c_g(\omega) < c_\phi(\Omega)]$. This behavior is illustrated on Fig. 3, where the temporal profiles of the acoustic particle velocity are plotted for several distances and for two limiting cases $p \ll 1$ and $p \gg 1$. The analysis has been carried out for the acoustic particle displacement but velocity temporal profiles are plotted here and in the following. The spectral transformation from the particle displacement to the particle velocity is simply done by an $i\Omega$ multiplication.

The widening of the Gaussian temporal profile of displacement corresponds to an integration of this profile, which ensures also an integration of the demodulated velocity profile, i.e., the transition from the first derivative of a Gaussian function to the derivative of zero order. This behavior has been predicted in Sec. III B 1, in the analysis of the two limiting cases $p \ll 1$, Eq. (31), and $p \gg 1$, Eqs. (33) and (34), for propagative pump waves. The occurrence of the term Ω in the denominator of expressions (33) and (34) ensures the demodulated temporal profile integration in the case $p \gg 1$. For $p \gg 1 (\omega \simeq 0.97, \Omega = 1.7\times10^{-3}, C = 5\times10^{-7})$ in Fig. 3, the integration of the velocity profile takes place between the observation distances $n=200$ and $n=7000$. Moreover, due to the asynchronism phenomenon, a saturation of the demodulated signal amplitude is observed starting from distances of several hundred beads. This is not the case when the velocity dispersion effects on the parametric antenna operation are negligible ($p \ll 1, \omega \simeq 0.083$ in Fig. 3). The demodulated signal amplitude in the latter case is not saturated in the range of the presented observation distances and the temporal profile remains unchanged, proportional to the first derivative of a Gaussian function.

B. Transition associated with the velocity dispersion

Without changing the observation distance of the demodulated signal, it is, however, possible to observe a transition in the shape of the demodulated velocity temporal profile by changing such parameters of the pump signal as the central frequency of the wave packet or the characteristic time of modulation of this packet $\tau_m \sim 1/\Omega$. In Fig. 4, such a transition is presented, for which the nondimensional parameter p is varied from $p \simeq 0.16$ to $p \simeq 12.2$ by increasing the carrier frequency of the Gaussian wave packet between $\omega \simeq 0.083$ and $\omega \simeq 0.97$. These limiting cases correspond to the expressions (31) and (32) of the transfer function $G(\omega, \Omega)$ of the self-demodulation process, respectively. For $p \ll 1$, $G(\omega, \Omega) \sim \omega^2 \ell_a(\omega)$, but for $p \gg 1$, $G(\omega, \Omega) \sim \omega^2 c_g(\omega)/\Omega[1-c_g(\omega)]$, which ensure an integration of the demodulated signal profile.

At the transition (integration of the velocity profile), the nondimensional parameter p is of the order of 1, which allows us to estimate the unknown parameter $\ell_a(\omega) \simeq c_g(\omega)/k(\Omega)[1-c_g(\omega)]$, because other variables (ω,Ω) are controlled.

It is important to notice that this transition $p \ll 1 \rightarrow p \gg 1$, obtained by increasing the carrier frequency ω, can also be done by increasing Ω (or by decreasing the characteristic modulation time of the pump wave packet $\tau_m \sim 1/\Omega$). The emergence of the latter transition for several values of the fixed carrier frequency ω should allow us to extract the dependence on ω of the pump wave intensity attenuation $\ell_a(\omega)$.

C. Transition propagative → evanescent pump waves

When the pump waves are no longer propagative but are localized in space near the HF emitter, the cumulative phenomena associated with the co-propagation of HF pump waves and LF demodulated waves dispppears. This singular modification in the pump wave transport might be a source of information about the medium, and particularly about its microstructure.

1. Case of two pump frequencies

The complete formula Eq. (19) is used to plot the demodulated signal amplitude as a function of the pump frequency in Fig. 5. The observation distance is fixed to $n=5000$, the attenuation constant is $C=5\times10^{-7}$, and the demodulated frequencies are equal to $\Omega \simeq 1.7\times10^{-4}$, 8.3×10^{-4}, 3.3×10^{-3}, 8.3×10^{-3}. For these four cases, a strong fall of the parametric antenna efficiency is observed around the cutoff frequency $\omega=1$ (between $\omega=0.9$ and $\omega=1.1$), typically from one to three orders of magnitude depending on Ω. When $\Omega \simeq 8.3\times10^{-3}$, an amplitude saturation effect due to the phase mismatch between the nonlinear sources and the demodulated wave occurs in the propagative zone $(\omega<1)$. This saturation effect is weaker for lower demodulated frequencies Ω. As a consequence, the efficiency fall, between, for instance, $\omega=0.9$ and $\omega=1.1$ is higher for $\Omega \simeq 1.7\times10^{-4}$ (more than three orders of magnitude) than for $\Omega \simeq 8.3\times10^{-3}$ (less than two orders of magnitude).

Similarly to the case $p \gg 1$ of Fig. 2, a pattern of minima and maxima is observed for the highest values of Ω in Fig. 5. The same phenomenon is responsible for this behavior, i.e., the velocity dispersion, which ensures an asynchronism between the nonlinear sources and the demodulated wave, being alternately in phase and out of phase. The formula, Eq. (45), allows us to find the minima, which gives, for $n=5000$ and $\Omega \simeq 8.3\times10^{-3}$, a first minimum at $\omega \simeq 0.37$. This result is in agreement with the corresponding curve, the black one in Fig. 5.

At the transition, $\omega=1$ and $k(\omega)=2/a$, which gives information on parameters like the contact stiffness α, the static stress applied on the chain, and the diameter of the beads a.

2. Case of a Gaussian pump wave packet

Concerning the signal profile demodulated from a Gaussian wave packet, its form can evolve in the transition between propagative pump waves and evanescent pump waves. In Fig. 6, three transitions are plotted for three values of the nondimensional parameter p, $p \gg 1$, $p \simeq 1$, and $p \ll 1$. Three carrier frequencies are used for each transition, $\omega \simeq 0.67$ and 0.83 (propagative) and $\omega \simeq 1.083$ (evanescent). The value of the attenuation constant remains unchanged, $C=10^{-6}$.

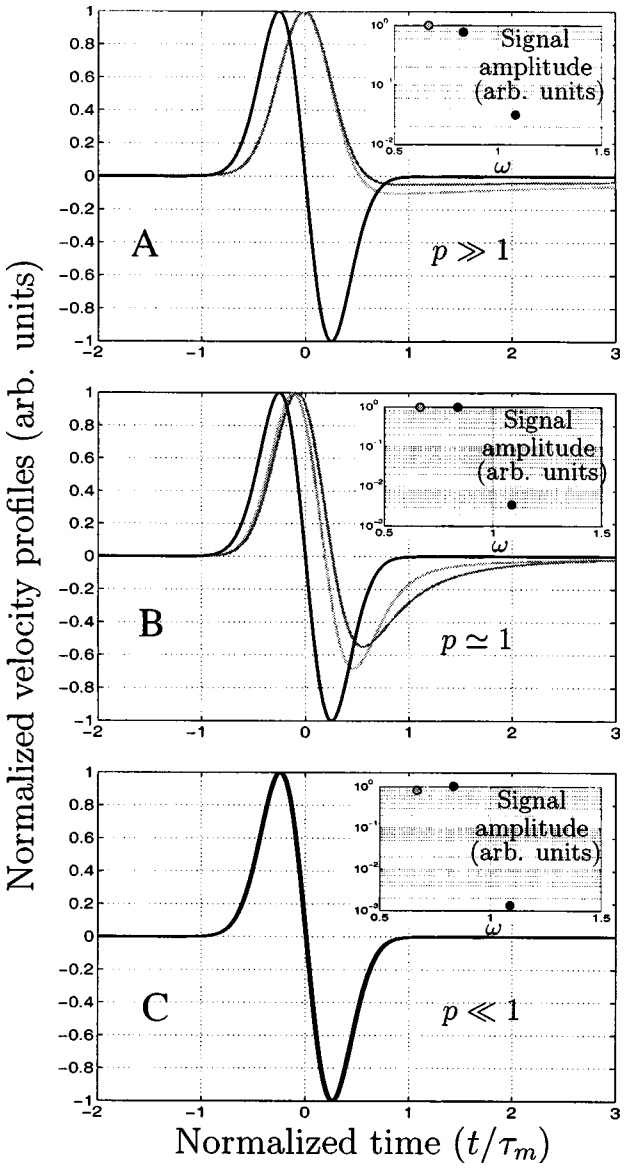

FIG. 6. Transition between the generation of the demodulated signal by propagative pump waves and by evanescent pump waves (out of the interaction region) for three values of the nondimensional parameter p. To give an estimation of the amplitude fall at the transition, the demodulated amplitudes are presented in the insets.

To vary the parameter p from $p \ll 1$ to $p \gg 1$, the characteristic modulation time of the pump wave packet is decreased from $\tau_m \simeq 8.3\times10^{-2}$ to $\tau_m \simeq 3.3\times10^{-5}$.

When $p \gg 1$, the modification of the profile associated with the transition between propagative and evanescent pump waves is represented in Fig. 6(a). As the effects of velocity dispersion in the propagative zone are significant [$p \gg 1$, limiting case (32)], the particle velocity profile is in-

tegrated and is proportional to a Gaussian function. The particle velocity profile demodulated from evanescent pump waves is proportional to the first derivative of a Gaussian when the carrier frequency is sufficiently greater than the cutoff frequency [see the limiting case (48)]. Thus, the transition from the propagative zone to the evanescent one manifests itself in this case by a derivation of the demodulated temporal profile. The associated inset shows a fall of at least one order of magnitude in the efficiency of the parametric antenna.

When $p \simeq 1$, the integration of the LF profile for propagative pump waves due to the velocity dispersion is partial. The transition in the shape of the profile still exists but is less clear than in the case $p \gg 1$. However, the signal being less saturated in amplitude due to a weaker influence of the velocity dispersion, the demodulated signal amplitude fall is greater than in the case $p \gg 1$ [see the inset of Fig. 6(b)].

Finally, when $p \ll 1$, no transition in the shape of the demodulated profile is observed. For both propagative and evanescent pump waves, the velocity profile is proportional to the first derivative of a Gaussian function [Fig. 6(c)]. It is, however, in this limiting case that the efficiency of the parametric antenna exhibits the deepest fall in amplitude between $\omega \simeq 0.83$ (propagative) and $\omega \simeq 1.083$ (evanescent), as is illustrated in the inset of Fig. 6(c). It has to be noticed that in this limiting case, the amplitude of the demodulated signal increases with the pump frequency practically all along the propagative zone, which is not the case for $p \gg 1$, where over a non-negligible region the transfer function $G(\omega, \Omega)$ decreases as a function of the pump frequency. In the evanescent zone, the demodulated amplitude decreases as a function of the pump frequency ω.

In conclusion, the transition between propagative and evanescent pump waves manifests itself, for $p \gg 1$, by a derivation of the demodulated profile and an efficiency fall of one order of magnitude. For $p \ll 1$, transformation of the profile is not predicted but there is a fall of efficiency of at least two orders of magnitude.

V. CONCLUSIONS

We have developed a theoretical model for the nonlinear self-demodulation process in a granular chain. This model takes into account the precise dispersion relation associated with the discrete nature of the lattice, and, in particular, accounts for the evanescent modes at high frequencies. By an integration of the analytically obtained LF displacement in the case of two primary frequencies, we have considered the self-demodulation of Gaussian wave packets. The dynamics of the LF demodulated wave amplitude is studied as a function of the primary wave frequency, the distance of propagation, and the absorption. The numerical results of Sec. IV were found to be in agreement with the analytical predictions of Sec. III not only qualitatively but also quantitatively (succession of minima and maxima in the demodulated amplitude as a function of pump wave frequency, for instance). Moreover, the theoretical analysis has shown that only a few parameters (p, P, etc.) are necessary to discriminate the different regimes of the parametric antenna operation in a granular chain.

The transition from propagative to evanescent primary waves manifests itself in each case by a strong decrease in the demodulated signal amplitude. In some particular cases, the shape of the temporal profile is also differentiated [Fig. 6(a) inset] when the primary waves become evanescent.

Velocity dispersion, through the asynchronism between HF nonlinear sources and LF demodulated waves, is saturating the self-demodulation process. Its manifestation is a pattern of maxima and minima in the amplitude dynamics of the LF demodulated wave in the case of two primary frequencies, or a saturation in amplitude and a pulse widening in the case of wide-frequency-band excitations.

It should be noted that although the transition from ballistics to diffusion, taking place with increasing frequency of the acoustic carrier wave in 3D irregular granular packing, leads to stronger localization of the acoustic energy near the emitter, similarly to the transition from propagative to evanescent mode transport in the 1D periodic granular chain studied above, its influence on the demodulation process is predicted to be quite different. The transition from propagative to evanescent pump waves manifests itself by a derivation of the demodulated wave pulse profile (this derivative can be partial or even absent in some cases), while the transition from ballistic to diffusion pump waves manifests itself by an integration of the demodulated pulse profile (this integration can be partial or even absent in some cases [27]).

ACKNOWLEDGMENT

This work was supported by DGA Contract No. 00.34.026.

[1] V. F. Nesterenko, J. Appl. Mech. Tech. Phys. **24**, 567 (1983).
[2] V. F. Nesterenko, J. Appl. Mech. Tech. Phys. **5**, 733 (1984).
[3] C. Coste, E. Falcon, and S. Fauve, Phys. Rev. E **56**, 6104 (1997).
[4] C. Coste and B. Gilles, Eur. Phys. J. B **7**, 155 (1999).
[5] C. H. Liu and S. R. Nagel, Phys. Rev. Lett. **68**, 2301 (1992).
[6] C. H. Liu and S. R. Nagel, Phys. Rev. B **48**, 15646 (1993).
[7] E. Hascoët, H. J. Herrmann, and V. Loreto, Phys. Rev. E **59**, 3202 (1999).
[8] M. de Billy, J. Acoust. Soc. Am. **108**, 1486 (2000).
[9] A. A. Maradudin, E. W. Montrell, G. H. Weiss, and I. P. Ipatova, *Theory of Lattice Dynamics in the Harmonic Approximation* (Academic, New York, 1971).
[10] Y. Nahmad-Molinari and J. C. Ruiz-Suarez, Phys. Rev. Lett. **89**, 264302 (2002).
[11] D. L. Blair *et al.*, Phys. Rev. E **63**, 041304 (2001).
[12] N. W. Mueggenburg *et al.*, Phys. Rev. E **66**, 031304 (2002).
[13] J. E. White, *Underground Sound Application of Seismic Waves*

(Elsevier, Amsterdam, 1983).
[14] K. L. Johnson, *Contact Mechanics* (Cambridge University Press, Cambridge, U.K., 1985).
[15] L. D. Landau and E. M. Lifshitz, *Theory of Elasticity* (Pergamon, Oxford, 1986).
[16] M. Manciu, S. Sen, and A. J. Hurd, Phys. Rev. E **63**, 016614 (2000).
[17] E. Hascoët and H. J. Hermann, Eur. Phys. J. B **14**, 183 (2000).
[18] S. Sen, M. Manciu, and J. D. Wright, Phys. Rev. E **57**, 2386 (1998).
[19] V. Y. Zaitsev, V. E. Nazarov, and V. I. Talanov, Acoust. Phys. **45**, 799 (1999).
[20] I. Y. Belyaeva, V. Y. Zaitsev, and E. M. Timanin, Acoust. Phys. **40**, 789 (1994).
[21] V. Y. Zaitsev, A. B. Kolpakov, and V. E. Nazarov, Acoust. Phys. **45**, 202 (1999).
[22] V. Y. Zaitsev, A. B. Kolpakov, and V. E. Nazarov, Acoust. Phys. **45**, 305 (1999).
[23] A-C. Hladky-Hennion, F. Cohen-Tenoudji, A. Devos, and M. de Billy, J. Acoust. Soc. Am. **112**, 850 (2002).
[24] L. Brillouin and M. Parodi, *Propagation des Ondes dans les Milieux Périodiques* (Masson, Paris, 1956).
[25] B. K. Novikov, O. V. Rudenko, and V. I. Timochenko, *Nonlinear Underwater Acoustics* (ASA, New York, 1987).
[26] F. Geniet and J. Leon, Phys. Rev. Lett. **89**, 134102 (2002).
[27] V. Tournat, V. E. Gusev, and B. Castagnède, Phys. Rev. E **66**, 041303 (2002).
[28] V. Tournat, B. Castagnède, V. E. Gusev, and P. Béquin, C. R. Mec. **331**, 119 (2003).